



Technical Sciences
Academy of Romania
www.jesi.astr.ro

Journal of Engineering Sciences and Innovation

Volume. 1, Issue 1 / 2016, pp. 73-89

*B. Electrotehnics, Electronics, Energetics,
Automation*

Received 8 April 2016

Accepted 3 September 2016

Received in revised form 23 June 2016

An integrated traffic and power grid simulator enabling the assessment of e-mobility impact on the grid: a tool for the implementation of the smart grid/city concept

**L. Bedogni¹, L. Bononi¹, A. Borghetti², R. Bottura², A. D'Elia¹,
M. Di Felice¹, F. Montori¹, F. Napolitano², C.A. Nucci^{2*},
T. Salmon Cinotti¹, F. Viola¹**

1. Department of Computer Science and Engineering, University of Bologna, Bologna, Italy

*2. Department of Electrical, Electronic and Information Engineering,
University of Bologna, Bologna, Italy*

Abstract. To successfully accomplish electro-mobility integration into city traffic, plans for the installation of adequate public charging infrastructures are of utmost importance. The assessment of the effects of the transients caused by the concurrent charging of a large number of electric vehicles to the operating conditions of the power network is part of such a planning development. The paper summarizes some of the work carried out in the authors' laboratories to accomplish such an assessment. In particular it describes the co-simulation platform integrating a) a mobility simulator suitably adapted to reproduce e-mobility in a typical middle-size Italian city center with b) a dynamic simulator of the power distribution network and with c) a simulator of a UMTS communication network, which has been developed to this purpose. The platform is shown to be able to support the development and performance test of specific countermeasures against power components overload, voltage variations and unbalances.

Keywords. Electric vehicle, charging stations, co-simulation, power distribution, vehicle routing.

1. Introduction

The smart grid represents the largest enabler for the implementation of the smart city paradigm. Of the several aspects relevant to the smart city concept, e-mobility is

* Correspondence address: carloalbertonucci@unibo.it; alberto.borghetti@unibo.it

increasingly getting importance. Within this context, charging infrastructures play a crucial role, as they can impact the operating conditions of electric power distribution networks, with particular reference to those serving urban areas. The assessment of the effects of the transients caused by the concurrent charging of a large number of electric vehicles to the operating conditions of the power network becomes therefore necessary in order to accomplish appropriate charging infrastructure planning and e-mobility integration into city traffic. The paper summarizes some of the work developed in the authors' laboratories to accomplish such an assessment [3]. More specifically it illustrates the structure of a co-simulation platform composed by the open source framework for vehicular traffic simulations VeinS [4], adapted to represent the main characteristics of electric vehicles (EVs) too and their charging requests, and a power distribution network model implemented in the EMTP-rv (Electromagnetic transient program) simulation environment [5], which includes the aggregate representation of clusters of electric vehicles supply equipment (EVSE) units. Moreover, in order to reproduce the flow of information and data required to properly manage the e-mobility integration into city traffic, the platform is interfaced with the communication network simulator Riverbed modeler (formerly called Opnet) [6], as described in [7], [8]. A Semantic Information Broker (SIB) is introduced to allow information storing and sharing among the different actors [9].

The impact of plug-in electrical vehicle charging on the electric power network has been recently presented in the literature in quite a few contributions, and different approaches in order to limit the negative effects and optimize the operating conditions of the system have been discussed (e.g. [10]–[19] and references therein). In this paper we focus on parking lots that include fast public charging stations with power rating assumed equal to 50 kW. The EVSE units of each parking lot are fed through a MV/LV transformer that represent the grid connection point (GCP). Following the hierarchical aggregation approach adopted in [13]–[15], we analyze a multi-agent system composed on the one hand by the intelligent electronic devices (IEDs) installed at the HV/MV substation and in correspondence of critical branches of the network that may be overloaded due to EVs charging and, on the other hand, by distributed agents, i.e. control units connected to the shared communication network, each associated to the cluster of EVSE units of a parking lot. The implemented distributed control algorithm allows the congestion management of the network whilst a local regulation function of the agents reduces the charging effects on voltage variations. Each agent communicates also with each single EVSE of the cluster in order to allocate the maximum power that could be absorbed from the MV network among the various charging EVs taking into account their specific characteristics and requirements. In this paper we assume that the multi-agent system (MAS) uses a third generation mobile cellular network, namely a Universal Mobile Telecommunication System (UMTS).

The paper is structured as follows: Section II illustrates the architecture of the co-simulation platform and its components, namely the traffic simulator and the power system simulator integrated through a semantic middleware. Further, the Section presents the main characteristics of the UMTS model adopted in this study.

Section III describes the MAS implemented in the simulator for the control of the EV charging stations. Section IV presents and discusses the simulation results relevant to transient simulations, whilst Section V is devoted to the analysis of the power flow profiles in the distribution network. Section VI concludes the paper.

2. The co-simulation platform

The three simulation environments on which the platform is based – traffic simulator, power distribution network simulator and communication network simulator – are described in what follows. Fig. 1 illustrates the data exchange among the three environments. The interface between the power distribution network simulator and the traffic simulator is realized leveraging the semantic capabilities of the SIB, as described in Fig. 2. Integration is carried out on 2 levels: time and data. Time integration is realized through a Web Server (WS) built in Python, having the role of a semaphore that controls the synchronization of the simulation flow. Data integration is obtained using the SIB, a semantic middleware originated by the European Project SOFIA and improved during the subsequent project related to electric mobility Internet of Energy (IOE) [20]. The SIB stores shared data coming from the two simulation sides in an interoperable format, allowing a bidirectional information flow. The semantic format used for the data representation is regulated by an ontology developed in the context of the IOE project, and has been chosen because it allows future extensions in an incremental way [21], [22].

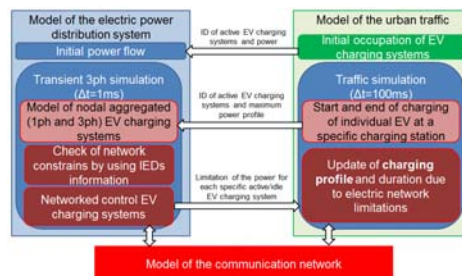


Fig. 1. Data exchange between the traffic simulator and the power distribution simulator.

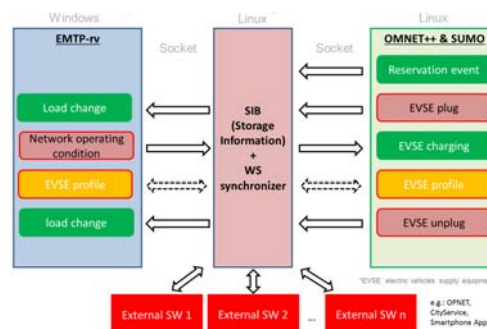


Fig. 2. Use of the SIB for the exchange of information and the WS for platform synchronization.

A. Traffic simulator

The urban traffic is modelled using VeinS, which is an open source framework for vehicular network simulations based on two simulators: OMNeT++, a discrete event-based simulator, and SUMO, a road traffic simulator. It has been extended with the models of EVs and EVSE units (including the management of the EVs queues) and has been integrated with the battery charging/discharging models described in [23]. For our analysis, we assumed a large-scale scenario (i.e. the downtown of Bologna), with a realistic street map (imported from the OpenStreetMap project).

B. Power distribution system simulator

The Power distribution system simulator is based on the Electromagnetic Transient Program EMTP-rv. It is a time domain simulator, in which we have adopted a time step of $\Delta t=1$ ms in all the simulations. The model of the distribution feeders includes the model of the three-phase unbalanced lines, three-phase HV/MV substation transformers equipped with an on-load tap changer (OLTC), and the models of the aggregated unbalanced loads (constant impedance / current / power) that includes the EVSE units.

The model of the EVSE aggregate is based on triplet of current sources, each controlled by a feed-back regulator in order to inject or absorb the requested per-phase values of active and reactive power as described in [7], [8]. Each aggregate load is connected at the secondary side of a MV/LV transformer.

The EMTP model includes a DLL (Dynamic Link Library)-based interface that allows the communication with the SIB.

C. Communication network simulator

The simulator of the UMTS communication network is based on the Riverbed Modeler Wireless suite v18.0 [6]. The Riverbed model includes the representation of the main components of the UMTS network: the user equipment (UE), i.e. the UMTS module of each agent, the Node B, the Radio Network Controller (RNC), which manages the Node B logical resources and the UE-Node B interface resources. The Serving GPRS support node (SGSN) maintains access controls, security functions and also keeps track of UE locations. Gateway GPRS support node (GGSN) encapsulates the packets and routes them to the SGSN that are received from the external network or Internet. The communication channels between each Node B and RNC are assumed wired with a large data rate.

The implemented model accounts for a block error rate (BLER), i.e. the percentage of transport blocks with errors over the total number of transport blocks. The Riverbed software supports the UMTS four main types of quality of service (QoS): background, interactive, streaming and conversational. These types of QoS are characterized by the traffic class, maximum and guaranteed bit rates, delivery order, transfer delay, maximum size of the service data unit (SDU) and SDU error ratio. The UE radio link control (RLC) interface could operate in either unacknowledged mode (UM) or acknowledged mode (AM), which includes retransmissions that decrease the effects of the BLER but increase the communication delay.

In this paper, the information exchanged between the agents uses the interactive QoS class communication that has higher priority than background QoS although, as background, it does not guarantee a bit rate. We have chosen to operate in AM.

In order to test the robustness of the control procedure against delays in the communication network, some simulations include a background traffic (BT) created by additional UEs, other than those associated with the agents. These new UEs and also the agents, generate the BT by using some default mobile user traffic profiles defined by Riverbed Modeler according to the 3GPP technical report TR 36.822. Since the analysis of the scheduling effects of the chosen QoS is out of the scope of this paper, also the BT is assumed to use the interactive QoS.

3. Multi agent system for the distributed control of charging stations

As mentioned in the Introduction, we assume to associate an agent to each cluster of EVSE units. The agent is able to adjust the EVSE charging powers. Moreover, we assume that intelligent electronic devices (IEDs) are installed at the HV/MV substation and at the feeder branches that may reach their maximum current rate during the operation of the distribution network. In particular, the presence of an IED at the beginning of each feeder connected to the secondary side of the HV/MV transformer is assumed. This IED measures the current and compares such a value with the maximum operation current value of the line. We also assume the presence of an IED able to detect the overload state of the HV/MV transformer.

Each IED is able to communicate an index over the UMTS cellular network that denotes whether and how much the corresponding power component is overloaded. In the literature this type of indexes are often called congestion prices (e.g., [11], [13]). The agent associated with each cluster of EVSEs is able to control the charging power according to the received congestion index.

The procedure implemented in the simulator is the following.

We assume that at time t , IED_{*j*} associated to the first branch of feeder j detects an overcurrent condition, i.e. $e_{j,t} = \frac{i_{j,t} - i_{j,\max}}{i_{j,\max}}$ greater than 1 where $i_{j,t}$ is the measured rms value of the current at time t and $i_{j,\max}$ is the maximum operating value. Then IED_{*j*} calculates the variation of the congestion index Δpr_j as

$$\Delta pr_{j,t} = K_c \left[(e_{j,t} - e_{j,t-1}) + \frac{\Delta t}{\tau_i} \left(\frac{e_{j,t} + e_{j,t-1}}{2} \right) \right] \quad (1)$$

where K_c and τ_i are constants, which are chosen equal to 0.2 and 0.1, respectively, in the simulations. Equation (1) corresponds to the velocity algorithm of a digital PI controller. Through the communication network, value $\Delta pr_{j,t}$ is sent by IED_{*j*} to the agents associated to clusters of EVSE units connected to feeder j . IED_{*j*} continues to perform calculation (1) until $\Delta pr_{j,t}$ becomes and stays constantly small enough or negative for at least a predefined settling time T_{set} chosen equal to 10 seconds. After T_{set} , $\Delta pr_{j,t}$ is set equal to 0. With a selected time step Δt (chosen equal to 1 s or 3 s in the simulations), the updated value of $\Delta pr_{j,t}$ is sent to the agents.

Each agent i that receives $\Delta pr_{j,t}$ at time t updates its own congestion index as

$$pr_{i,t} = \max(1, pr_{i,t-1} + \Delta pr_{j,t}) \quad (2)$$

and fixes the maximum power that could be absorbed by the relevant cluster of EVSEs as

$$P_{EVSE_{i,t}} = \frac{\widehat{P}_{EVSE_{i,t}}}{pr_{i,t}} \quad (3)$$

where $\widehat{P}_{EVSE_{i,t}}$ is the maximum power requested by the EVSEs of the cluster associated to agent i at time t .

Compared with the broadcast of congestion indexes, the velocity form of the control mechanism provided by (1) avoids reset windup and, in (2), it permits to sum the contributions of various IEDs that detect the concurrent overload of different power components.

Each agent i also includes a local voltage regulator that proportionally reduces $P_{EVSE_{i,t}}$ if the local voltage at the MV side of the transformer is lower than a predefined value (e.g., 0.97 pu).

4. Simulation results

In this section we describe the simulation results obtained with the described platform. Fig. 3 shows the locations of parking lots with EVSE units in Bologna. We focus here to two 15 kV feeders fed by 132/15 kV substation SB_A (indicated in red in Fig. 3), to which four clusters of 50 kW EVSE units are assumed to be connected, namely EVSE_1 and EVSE_2 to feeder 1, EVSE_3 and EVSE_4 to feeder 2. Fig. 3 also shows the main components of the implemented model of the UMTS communication network, assuming that all the four agents each associated to a cluster are served by the same Node B.

The traffic simulator generates a flow of random events. Each event represents a specific trip of a vehicle in the city from a starting point to a destination. For the case of EVs, when the state of charge (SOC) of the corresponding battery is below a threshold set to 25%, the vehicle deviates from the planned journey and reaches the closest EVSE unit available.

The EMTP model represents the two 15 kV feeders of interest with the relevant loads, the 132/15 kV transformer of the HV/MV substation and the equivalent impedance of the HV network. It includes also the model of three-phase loads (assumed constant for these simulations) and the aggregate EVSE models of clusters EVSE_1, EVSE_2, EVSE_3, and EVSE_4, each fed through a 15/0.4 kV transformer. Moreover the EMTP model represents both the IEDs and the agents that communicate between each other and the SIB through the DLL interface.

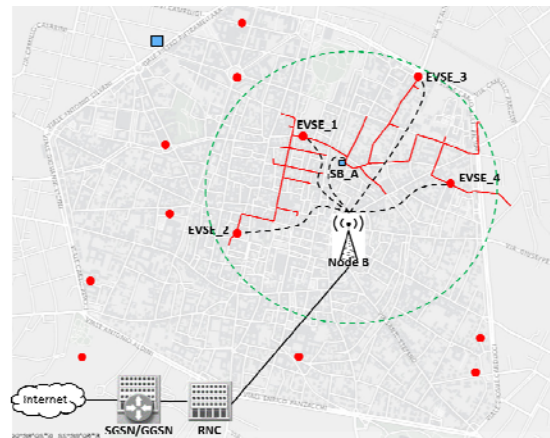


Fig. 3. Top view of the map of Bologna with the indication of parking lots with EVSE clusters (red dots), of HV/MV substations (blue rectangles), the analyzed two 15kV feeders and the model of the UMTS communication network (dotted black lines represent wireless channels, solid black lines represent wired channel). The green circle indicates the estimated coverage areas of the Node B antenna.

The results presented here refer to a simulation that starts with a random generation of 200 events, each one every 5 seconds. With a 50% uniform probability each event is associated with an EV, otherwise is represented by a fuel vehicle. Every time a vehicle leaves the simulation, i.e. reaches its destination, a new event is generated. For illustrative purpose, the EVs are generated with a SoC below the minimum threshold.

EMTP is linked and synchronized with VeinS after 400 s of traffic generation.

The simulations are repeated for two different BLER values: $1E^{-5}$ (case indicated as BLER0) and 0.1 (BLER1), which is a typical reference performance value (e.g. [24]).

Moreover, the same simulations are repeated with the BT (case indicated as BT1) and without the BT (BT0). BT is generated by the UEs associated to the agents and by seven additional UEs and two traffic receivers. The two adopted mobile users application models are characterized by two different gamma distributions of the inter-arrival packet time in s (with parameters 0.0068, 5 and 0.2, 0.5, respectively) and exponential distributions of packet size in bytes (with parameters 41.03 and 62.97, respectively).

Fig. 4 shows the dynamic change of the number of vehicles that are connected to an EVSE of each of the four considered clusters, whilst Fig. 5 and Fig. 6 show the requested power by each of the clusters and the current measured at the beginning of the two feeders. The current value of 1 pu indicates the maximum allowed operating value (in the considered feeders it is equal to 200 A).

As shown by Fig. 6, after 420 s since the beginning of the EMTP simulation, the IEDs associated to the initial branch of the two feeders detect an overcurrent condition. They calculate the variation of the congestion indexes according to (1) and send them at each $\Delta t = 1$ s to the agents of the relevant EVSE clusters. Fig. 7 shows the sent values of the congestion index variations, whilst Fig. 8 shows the congestion

index values independently calculated by each of the agents of the four EVSE clusters by using (2). The congestion index is used by the agents in order to limit the EVSE power according to (3). Fig. 5 shows the limitation of the absorbed power by each EVSE cluster, whilst Fig. 6 shows the effectiveness of the control action that is able to promptly compensate the overloading conditions caused by each new connection of an EV to an EVSE.

As can be seen from Fig. 5 and Fig. 8, the control without communication interference and packet loss, the final power requested and congestion index by the clusters connected to the same feeder is equal. With delay and loss of information, this fairness condition is no longer verified and these values differ from each other by 9.3 kW for EVSE_1 and EVSE_2 (feeder 1) and by 4.8 kW for the EVSE_3 and EVSE_4 (feeder 2).

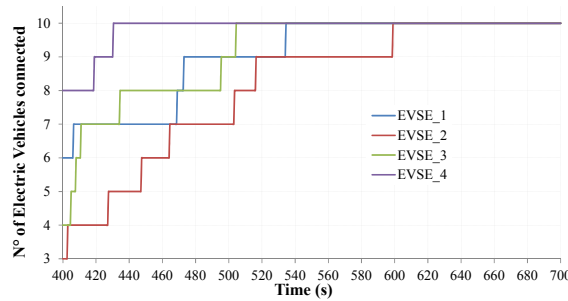


Fig. 4. Number of EVs in charge in each of the considered clusters.

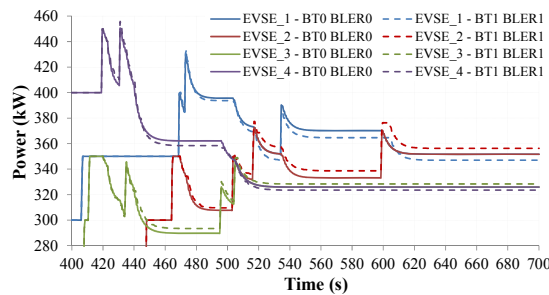


Fig. 5. Power requested by each EVSE cluster ($\Delta t = 1$ s).

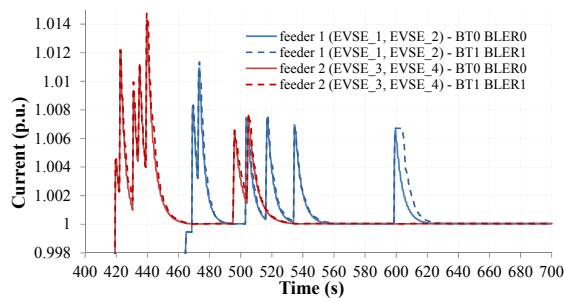


Fig. 6. Current value measured by the IEDs associate to the first branch of the two considered feeders ($\Delta t = 1$ s).

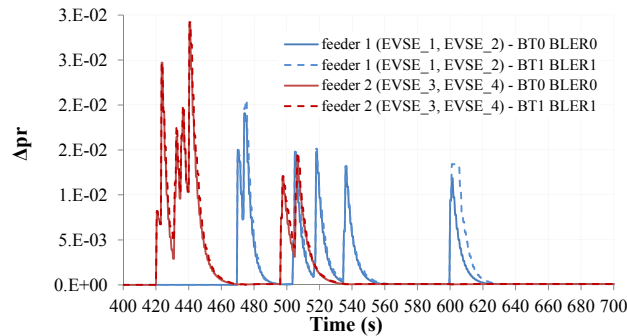


Fig. 7. Congestion index variations sent by the two IEDs to the agents ($\Delta t = 1$ s).

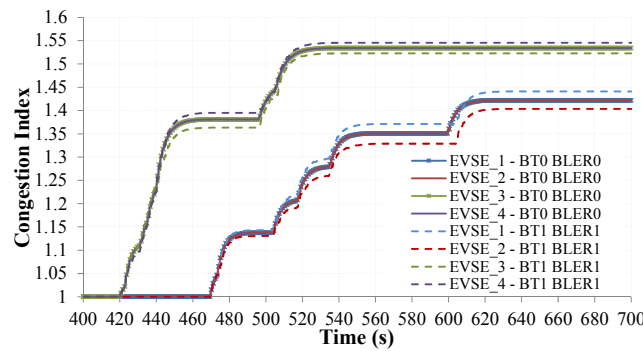


Fig. 8. Congestion indexes independently calculated by each agent of an EVSE cluster ($\Delta t = 1$ s).

The simulations have repeated for $\Delta t = 3$ s. Analogously to the previous figures, Fig. 9, Fig. 10, Fig. 11 and Fig. 12 show the power requested by each EVSE cluster, the measured currents, the congestion index variations and the congestion indexes calculated by each agents. The results refer to the same sequence of connection of EVs shown in Fig. 4 and they are repeated for both the case of ideal communication and the case with both BLER and BT.

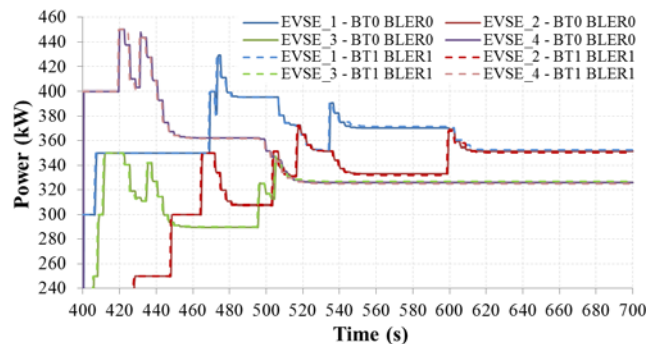


Fig. 9. Power requested by each EVSE cluster ($\Delta t = 3$ s).

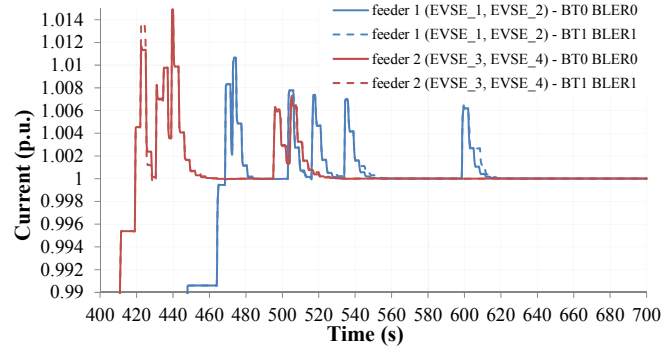


Fig. 10. Current value measured by the IEDs associate to the first branch of the two considered feeders ($\Delta t = 3$ s).

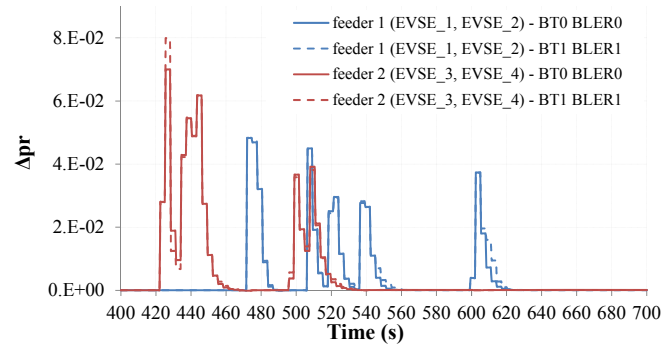


Fig. 11. Congestion index variations sent by the two IEDs to the agents ($\Delta t = 3$ s).

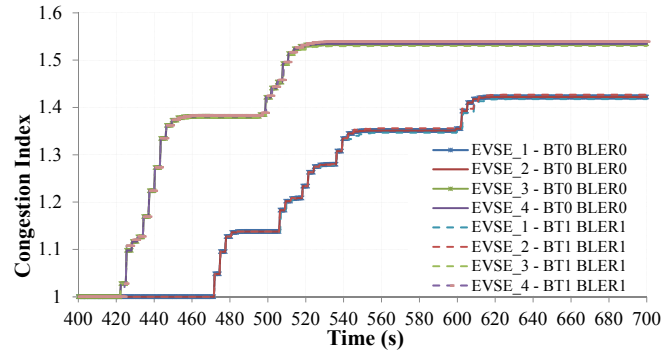


Fig. 12. Congestion indexes independently calculated by each agent of an EVSE cluster ($\Delta t = 3$ s).

Table I shows additional details on the results: the total overloading duration during which the currents measured by the two IEDs, indicated as I_1 and I_2 , exceed the maximum value, the maximum current measured by each IEDs, the mean and standard deviation of the delay of the communication packets and the correspondent number of packet transmitted and received. As expected, for the case of communication affected by BLER and BT, both the mean value and standard deviation of packet delays are larger than in the case of ideal communication. Moreover BLER causes the loss of some packets. The use of $\Delta t = 3$ s limits the number of packets and reduces the influence of both packet delay and packet loss.

Table 1 Time above the current limit, packet delay and Number of packets (Tx: transmitted, Rx: received)

BT BLER	Time $I_1 > 1\text{pu}$ (s)	Time $I_2 > 1\text{pu}$ (s)	I_1 max (p.u.)	I_2 max (p.u.)	Packet delay (ms) mean (stdev)	Number of pack- ets TX RX
BT0 BLER0 $\Delta t = 1$ s	93	79	1.0109	1.0143	142.6 (10.0)	378 378
BT1 BLER1 $\Delta t = 1$ s	101	81	1.0113	1.0147	231.3 (189.0)	406 363
BT0 BLER0 $\Delta t = 3$ s	71	69	1.0107	1.0149	149.7 (12.7)	122 122
BT1 BLER1 $\Delta t = 3$ s	81	69	1.0107	1.0149	235.3 (180.5)	128 120

As shown by figures and the Table, the overall performance of the implemented control strategy is not significantly affected by the presence of BLER and BT. The difference between the results obtained for $\Delta t = 1$ s and $\Delta t = 3$ s is not significant.

5. Analysis of the power flow profiles in the distribution network

In order to calculate the expected power flows in the distribution network at different times of the day in different operating conditions taking into account the effects of electric vehicle charging processes, we have included the representation of an ideal congestion management procedure in a power flow calculation code. The main simplifying assumption is that the communication between the IEDs and the agents located at the parking lots is instantaneous and without data loss.

This section at first describes the representation of the ideal congestion management strategy, then it provides some results relevant to the average power drained by EVSEs over a day.

As already mentioned, each cluster of EVSEs (e.g. those inside a parking lot) is fed through a grid connection point (GCP). The analysis of the power flow profiles is carried out by a sequence of power flow calculations, one for each time a variation in the system occurs. Each time a load flow analysis is performed, the following procedure calculates, for each GCP_{*i*}, the power variation ΔP_i needed in order to compensate the congestion detected by an IED located upstream. The value of $I_{\text{max, IED}}$ is known as it is the maximum value above which the IED will detect a condition of congestion. Moreover, the following values are obtained from the power flow calculation:

- $I_{\text{IED}} = I_{\text{re, IED}} + j \cdot I_{\text{im, IED}}$ is the phasor of the current measured by the IED, being j the imaginary unit.

- V_i is the RMS value of the voltage phasor at GCP_i .
- θ_i is the phase of the voltage phasor at GCP_i .
- P_i is the active power absorbed by GCP_i .

For each GCP_i , the total RMS variation of the current to be absorbed is calculated as:

$$\Delta I_i = \frac{P_i}{\sum P_i} \left[-\tilde{I}_i + \sqrt{\tilde{I}_i^2 - (|I_{IED}|^2 - I_{max,IED}^2)} \right] \quad (4)$$

where

$$\tilde{I}_i = (I_{re,IED} \cos \theta_i + I_{im,IED} \sin \theta_i) \quad (5)$$

and $\sum P_i$ involves all the GCP_i connected downstream to the location of the considered IED. If more than one IED is located upstream to a GCP, then the maximum value of ΔI_i is considered. Equation (4) has been obtained by assuming that the needed corrections are small at each step and, therefore, the variations of the losses in the network as well as the variations of the current absorptions and injections of all the loads and generators connected to the network due to voltage deviations can be neglected. The value of active power variation ΔP_i at GCP_i is calculated from ΔI_i and V_i . If there are congestions, then ΔP_i is positive and each GCP_i located downstream the relevant IED should reduce the power used by each EVSE fed by GCP_i for a total power equal to ΔP_i . If there is no congestion, ΔP_i is negative, thus each downstream GCP_i is allowed to increase the power requested by up to $|\Delta P_i|$.

Given ΔP_i as the power reduction for a single GCP_i , the typical objectives for the allocation of the power variations requested among all the EVSEs fed by such GCP are:

- 1) maximize the revenue for the owner of the EVSEs;
- 2) maximize the number of vehicles fully recharged;
- 3) maximize the energy given to each vehicle connected within the same GCP, being as fair as possible.

Considering objective 2, some vehicles can be nearly empty at the end of the process because some other vehicles have profited of a higher priority. For such reason, we consider objective 3 for the purpose of the simulation. Electric vehicles drivers can behave basically in two different ways, which can affect significantly the choice of the redistribution algorithm:

- a) book the EVSE for the minimum time required to get the battery fully recharged assuming to get the maximum power (e.g. a driver in a hurry);
- b) book the EVSE for a long time (some hours) to enable slow recharge when the demand is high (e.g. a driver that parks the car close to his or her workplace). Such behavior can depend on further policies.

In this paper we consider a) by implementing an earliest deadline first logic, which gives the maximum power to vehicles with the earliest deadline. Moreover each EVSE of the same parking lot is requested decreases power by the same amount. The effects are presented in the following simulation results.

Our scenario simulates the downtown of Bologna, including a realistic mobility dataset [25], used for geographic purposes. However, the mobility traces provided in such work are valid for just one hour of traffic, while we aim to simulate the traffic over a regular weekday. For this reason, we generated the routes through the tool SUMO-Duarterouter with respect to available statistics on the traffic rate shown in Figure 13. In particular, the ratio of vehicles running at the same time is shown at different times of the day, for which we considered a total number of 30000. The traffic is represented by a pool of 10000 different routes and we introduce dynamically a vehicle every time the total number is below the number expected. Similarly, a vehicle is deleted when the effective number is beyond the threshold. Whenever a new vehicle is generated, it is randomly assigned to be electric or fuel-propelled according to the established ratio of PEVs in the traffic. In our case, we ran simulations considering the 5% and the 10% of the vehicles to be electric. Furthermore, each PEV is generated with a uniformly random SOC between 0.2 and 0.8. Vehicles reaching a SOC under a threshold start to look for an available EVSE using the reservation mechanism. Such a threshold is set to a random value between 0.08 and 0.12.

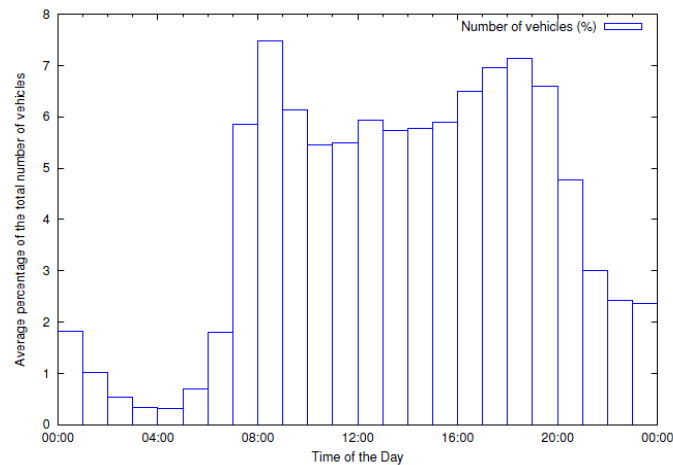


Fig. 13. Vehicle rate throughout the day.

The power distribution network is the same already described in Section IV. We refer to the normal urban loads (excluding EVSEs) as “city loads” and we model their power drain throughout the day using the curve shown in Figure 14, applying the ratio of power drained to their nominal value using a Gaussian error.

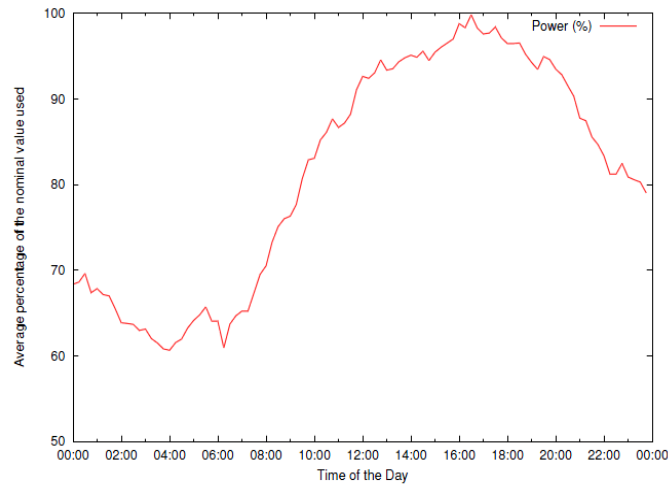
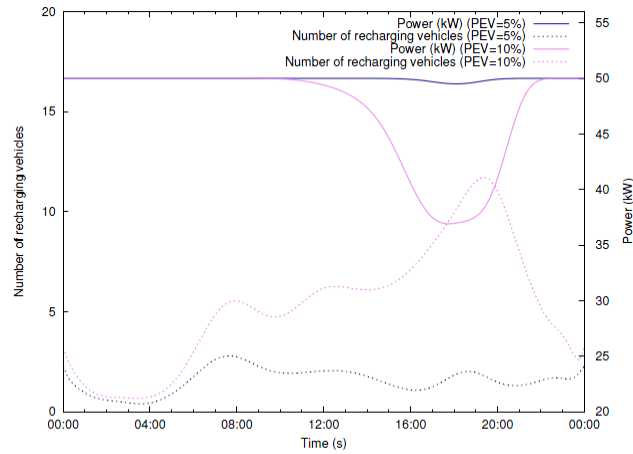
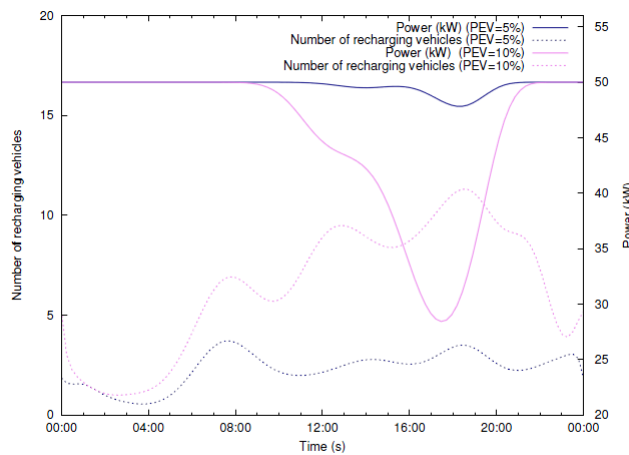


Fig. 14. Average percentage of power drained by a “city load” throughout the day compared to its nominal value

Several daily simulations have been performed assuming all the parameters described above, monitoring both the number of vehicles recharging at the same time and the average power drained by each EVSE. Results present a high variance, due to the random selection of the free EVSE where to recharge. Example of results are shown in Figure 15(a) for IED1 and Figure 15(b) for IED2. We observed that, in such conditions, load peaks are occurring as expected during several concurrent recharging processes, however it is strongly dependent on the time of the day, reaching a critical peak at around 6 PM. In particular it is shown that at 8 AM, when the traffic density is very high and we would expect an overload, the distribution grid succeeds to handle such a demand, whilst in the evening the maximum power available for each EVSE is reduced by the DAs. It is also evident that parking lots fed by GCPs downstream to IED1 tend to be less preferred by drivers compared to IED2, due to the parking lot closeness to important zones for the urban traffic. In addition, due to the power network configuration and the city loads distribution, IED1 is, in general, advantaged when considering an equal number of recharging vehicles. Furthermore, diagrams show that doubling the number of PEVs (from 5% to 10%) results in a much more serious issue for the grid. In fact, while an amount of PEVs equal to 5% of the traffic causes small losses of power for the EVSEs, a number of PEVs of 10% causes sometimes the average power for an EVSE to be nearly halved. This is also due to the waiting queues at the EVSEs, causing the number of recharging vehicles to rise in the subsequent hours.



(a) IED1



(b) IED2

Fig. 15. Vehicle rate throughout the day.

6. Conclusions

The paper reports some of the results relevant to a specifically developed co-simulation platform for to the analysis of the impact of electric mobility on the operation of the urban power distribution network.

The simulation results show the effectiveness of a congestion management approach based on a multi-agent system in which IEDs installed both at the HV/MV substation and at the feeder branches that may reach their maximum current rate communicates congestion indexes variations to the agents that control the EVSE clusters.

The analysis has been carried out taking care of the communication network constraints. In particular the co-simulation platform incorporates a model of a mobile cellular network. Latency and communication errors do not appear to significantly

affect the control scheme performance although equal allocation of the control effort among different EVSE clusters connected to the same feeder is reached only in the case of ideal communication.

The calculation of the daily load profiles taking into account the request from public aggregates of electric vehicle charging stations allows the detection of the periods of the day and the parts of the power distribution network associated with the highest risk of congestions.

Acknowledgments

The Authors thank Marco Di Felice, Mathias Duckheim, Randolf Mock and Luca Roffia for helpful comments and suggestions. Riverbed software has been used thanks to the Riverbed University Program.

References

- [1] L. Bedogni, L. Bononi, A. Borghetti, R. Bottura, A. D. Elia, and T. S. Cinotti, "Integration of traffic and grid simulator for the analysis of e-mobility impact on power distribution networks," in *2015 IEEE Eindhoven PowerTech*, 2015, pp. 1–6.
- [2] F. Montori, A. Borghetti, and F. Napolitano, "A Co-Simulation Platform for the Analysis of the Impact of Electromobility Scenarios on the Urban Distribution Network," in *2nd International Forum on Research and Technologies for Society and Industry (RTSI 2016)*, 2016, pp. 1–6.
- [3] A. D'Elia, F. Viola, F. Montori, M. Di Felice, L. Bedogni, L. Bononi, A. Borghetti, P. Azzoni, P., D. Tarchi, R. Mock, and T. S. Cinotti, "Impact of Interdisciplinary Research on Planning, Running, and Managing Electromobility as a Smart Grid Extension," *IEEE Access*, vol. 3, pp. 2281–2305, 2015.
- [4] C. Sommer, R. German, and F. Dressler, "Bidirectionally Coupled Network and Road Traffic Simulation for Improved IVC Analysis," *IEEE Trans. Mob. Comput.*, vol. 10, no. 1, pp. 3–15, Jan. 2011.
- [5] J. Mahseredjian, S. Denetiere, L. Dubé, B. Khodabakhchian, and L. Gérin-Lajoie, "On a new approach for the simulation of transients in power systems," *Electr. Power Syst. Res.*, vol. 77, no. 11, pp. 1514–1520, Sep. 2007.
- [6] "OPNET-Riverbed Modeler Wireless suite v18.0." .
- [7] R. Bottura, A. Borghetti, F. Napolitano, and C. A. Nucci, "ICT-power co-simulation platform for the analysis of communication-based volt / Var optimization in distribution feeders," in *5th Innovative Smart Grid Technologies Conference ISGT*, 2014, pp. 1–5.
- [8] R. Bottura and A. Borghetti, "Simulation of the volt/var control in distribution feeders by means of a networked multi-agent system," *IEEE Trans. Ind. Informatics*, vol. 10, no. 4, pp. 2340–2353, 2014.
- [9] F. Morandi, L. Roffia, A. D'Elia, F. Vergari, and T. Salmon Cinotti, "RedSib: a Smart-M3 semantic information broker implementation," in *Proc. 12th Conf. of Open Innovations Association FRUCT and Seminar on e-Tourism*, 2012, pp. 86–98.
- [10] N. Rahbari-Asr and M.-Y. Chow, "Cooperative Distributed Demand Management for Community Charging of PHEV/PEVs Based on KKT Conditions and Consensus Networks," *IEEE Trans. Ind. Informatics*, vol. 10, no. 3, pp. 1907–1916, Aug. 2014.
- [11] O. Ardakanian, S. Keshav, and C. Rosenberg, "Real-Time Distributed Control for Smart Electric Vehicle Chargers: From a Static to a Dynamic Study," *IEEE Trans. Smart Grid*, vol. 5, no. 5, pp. 2295–2305, Sep. 2014.
- [12] Z. Ma, D. S. Callaway, and I. A. Hiskens, "Decentralized Charging Control of Large Populations of Plug-in Electric Vehicles," *IEEE Trans. Control Syst. Technol.*, vol. 21, no. 1, pp. 67–78, Jan. 2013.
- [13] M. D. Galus, R. A. Waraich, F. Noembrini, K. Steurs, G. Georges, K. Boulouchos, K. W. Axhausen, and G. Andersson, "Integrating Power Systems, Transport Systems and Vehicle Technology for Electric Mobility Impact Assessment and Efficient Control," *IEEE Trans. Smart Grid*, vol. 3, no. 2, pp. 934–949, Jun. 2012.

-
- [14] E. L. Karfopoulos and N. D. Hatziaargyriou, "A Multi-Agent System for Controlled Charging of a Large Population of Electric Vehicles," *IEEE Trans. Power Syst.*, vol. 28, no. 2, pp. 1–1, 2012.
- [15] C.-K. Wen, J.-C. Chen, J.-H. Teng, and P. Ting, "Decentralized Plug-in Electric Vehicle Charging Selection Algorithm in Power Systems," *IEEE Trans. Smart Grid*, vol. 3, no. 4, pp. 1779–1789, Dec. 2012.
- [16] S. Deilami, A. S. Masoum, P. S. Moses, and M. A. S. Masoum, "Real-Time Coordination of Plug-In Electric Vehicle Charging in Smart Grids to Minimize Power Losses and Improve Voltage Profile," *IEEE Trans. Smart Grid*, vol. 2, no. 3, pp. 456–467, Sep. 2011.
- [17] L. Pieltain Fernandez, T. Gomez San Roman, R. Cossent, C. Mateo Domingo, and P. Frias, "Assessment of the Impact of Plug-in Electric Vehicles on Distribution Networks," *IEEE Trans. Power Syst.*, vol. 26, no. 1, pp. 206–213, Feb. 2011.
- [18] E. Sortomme, M. M. Hindi, S. D. J. MacPherson, and S. S. Venkata, "Coordinated Charging of Plug-In Hybrid Electric Vehicles to Minimize Distribution System Losses," *IEEE Trans. Smart Grid*, vol. 2, no. 1, pp. 198–205, Mar. 2011.
- [19] K. Clement-Nyns, E. Haesen, and J. Driesen, "The Impact of Charging Plug-In Hybrid Electric Vehicles on a Residential Distribution Grid," *IEEE Trans. Power Syst.*, vol. 25, no. 1, pp. 371–380, Feb. 2010.
- [20] "Internet of Energy project (IOE)." [Online] . Available: <http://www.artemis-ioe.eu/>.
- [21] J. Honkola, H. Laine, R. Brown, and O. Tyrkko, "Smart-M3 information sharing platform," in *The IEEE symposium on Computers and Communications*, 2010, pp. 1041–1046.
- [22] E. Ovaska, T. Salmon Cinotti, and A. Toninelli, "The design principles and practices of interoperable smart spaces," in *Advanced design approaches to emerging software systems*, X. Liu and Y. Li, Eds. Hershey PA: IGI Global, 2011, pp. 18–47.
- [23] L. Bedogni, L. Bononi, M. Di Felice, A. D'Elia, R. Mock, F. Montori, F. Morandi, L. Roffia, S. Rondelli, T. S. Cinotti, and F. Vergari, "An interoperable architecture for mobile smart services over the internet of energy," in *2013 IEEE 14th International Symposium on "A World of Wireless, Mobile and Multimedia Networks" (WoWMoM)*, 2013, pp. 1–6.
- [24] Mishra A.R., Ed., *Advanced Cellular Network Planning and Optimisation: 2G/2.5G/3G...Evolution to 4G*. John Wiley & Sons, 2007.
- [25] L. Bedogni, M. Gramaglia, A. Vesco, M. Fiore, J. Härri, and F. Ferrero, "The Bologna Ringway Dataset : Improving Road Network Conversion in SUMO and Validating Urban Mobility via Navigation Services," vol. 64, no. 12, pp. 5464–5476, 2015.